

A Methodological Approach to Non-invasive Assessments of Vascular Function and Morphology

Sandoo, A.; Kitas, G.D.

Journal of Visualized Experiments

DOI:
[10.3791%2F52339](https://doi.org/10.3791%2F52339)

Published: 02/07/2015

Publisher's PDF, also known as Version of record

[Cyswllt i'r cyhoeddiad / Link to publication](#)

Dyfyniad o'r fersiwn a gyhoeddwyd / Citation for published version (APA):
Sandoo, A., & Kitas, G. D. (2015). A Methodological Approach to Non-invasive Assessments of Vascular Function and Morphology. *Journal of Visualized Experiments*, 96, e52339.
<https://doi.org/10.3791%2F52339>

Hawliau Cyffredinol / General rights

Copyright and moral rights for the publications made accessible in the public portal are retained by the authors and/or other copyright owners and it is a condition of accessing publications that users recognise and abide by the legal requirements associated with these rights.

- Users may download and print one copy of any publication from the public portal for the purpose of private study or research.
- You may not further distribute the material or use it for any profit-making activity or commercial gain
- You may freely distribute the URL identifying the publication in the public portal ?

Take down policy

If you believe that this document breaches copyright please contact us providing details, and we will remove access to the work immediately and investigate your claim.

Video Article

A Methodological Approach to Non-invasive Assessments of Vascular Function and Morphology

Aamer Sandoo^{1,2}, George D. Kitas^{2,3}

¹School of Sport, Health and Exercise Sciences, Bangor University

²Department of Rheumatology, Dudley Group of Hospitals NHS Trust, Russells Hall Hospital

³Arthritis Research UK Epidemiology Unit, University of Manchester

Correspondence to: Aamer Sandoo at aamer.sandoo@nhs.net

URL: <http://www.jove.com/video/52339>

DOI: [doi:10.3791/52339](https://doi.org/10.3791/52339)

Keywords: Medicine, Issue 96, Endothelium, Cardiovascular, Flow-mediated dilatation, Carotid intima-media thickness, Atherosclerosis, Nitric oxide, Microvasculature, Laser Doppler Imaging

Date Published: 2/7/2015

Citation: Sandoo, A., Kitas, G.D. A Methodological Approach to Non-invasive Assessments of Vascular Function and Morphology. *J. Vis. Exp.* (96), e52339, doi:10.3791/52339 (2015).

Abstract

The endothelium is the innermost lining of the vasculature and is involved in the maintenance of vascular homeostasis. Damage to the endothelium may predispose the vessel to atherosclerosis and increase the risk for cardiovascular disease. Assessments of peripheral endothelial function are good indicators of early abnormalities in the vascular wall and correlate well with assessments of coronary endothelial function. The present manuscript details the important methodological steps necessary for the assessment of microvascular endothelial function using laser Doppler imaging with iontophoresis, large vessel endothelial function using flow-mediated dilatation, and carotid atherosclerosis using carotid artery ultrasound. A discussion on the methodological considerations for each of the techniques is also presented, and recommendations are made for future research.

Video Link

The video component of this article can be found at <http://www.jove.com/video/52339/>

Introduction

The endothelium is the innermost lining of the vasculature and is involved in the maintenance of vascular homeostasis via the regulation of a multitude of vasoactive processes. Disruption to these processes may predispose the vessel to atherosclerosis and increase the risk for cardiovascular disease (CVD) ¹. Peripheral endothelial function is a good indicator of early abnormalities in the vascular wall ². Furthermore, measures of peripheral endothelial function have been shown to reflect coronary endothelial function ³⁻⁵, and as such are regarded as good predictors of cardiovascular disease ⁶⁻⁹. This is perhaps hardly surprising given that atherosclerosis is now broadly appreciated to be a systemic disorder ¹⁰. Assessments of peripheral endothelial function typically quantify the vasodilatory response of the vessel to a specific stimulus, with an attenuation of the dilatory response indicative of endothelial dysfunction ¹¹, and can be measured in different vascular beds. Assessments of advanced structural changes in the vessel can be characterised by ultrasound examination of the intima-media thickness.

In the microcirculation, laser Doppler flowmetry (LDF) and Laser Doppler imaging (LDI) with iontophoresis of vasodilator agonists can provide useful information on microvascular perfusion ¹². Both techniques measure the Doppler shift created by scattered light from moving red blood cells. Perfusion is represented as blood flux rather than blood flow (ml/min), with blood flux reflecting average red blood cell velocity and concentration. Measurement of blood flux is linearly associated with actual blood flow ¹³. The assessment of LDI offers considerable advantages over LDF, because unlike LDF, LDI can scan over a vast area thus accounting for heterogeneity in skin blood flow and increasing the reproducibility of the technique ¹².

The stimulus for increasing blood flux during LDI are provided by iontophoresis of vasodilator agonists acetylcholine (ACh) and sodium nitroprusside (SNP), which assess endothelium-dependent and endothelium-independent function respectively, into the skin using a weak electrical current ¹⁴. Once through the skin, ACh binds to endothelial cell muscarinic receptors releasing the vasodilator nitric oxide (NO). The use of SNP directly activates smooth muscle cell receptors to allow for maximum vasodilatation of the vessel and examination of smooth muscle integrity ¹⁵. There is some uncertainty on whether ACh-mediated dilatation involves NO at all, as ACh may stimulate non-NO pathways such as cyclooxygenase-mediated pathways ¹². Nevertheless, we have previously reported that ACh and SNP responses are impaired in patient populations at increased risk of CVD ¹⁶ and that exercise interventions known to improve NO bioactivity also improve ACh-mediated blood flux using LDI ¹⁷. The vehicle for transporting the agents into the skin microvessels often include sodium chloride or deionised water ^{18,19}. Microvascular endothelial function can be quantified using different approaches, with cutaneous vascular conductance – a product of flux divided by arterial pressure, used in studies where blood pressure may change over the study duration (*i.e.*, during exercise or anti-hypertensive treatment) ¹². Another commonly used quantification is to calculate the area under the curve for blood flux or express the percentage increase in

flux from baseline. It is important to note that there are no established guidelines for presenting data, but investigators should utilise an approach which shows good reproducibility.

In the large vessels, flow-mediated dilatation (FMD) and glyceryl-trinitrate mediated dilatation (GTN) are performed to assess endothelium-dependent and endothelium-independent function respectively²⁰. FMD is typically carried out in the brachial artery where a cuff is used to occlude arterial blood flow for 5 min; release of the cuff causes a sudden increase in blood flow (reactive hyperaemia) through the brachial artery resulting in shear-stress mediated dilatation of the vessel. The baseline and post-cuff release diameter are quantified by ultrasound imaging of the vessel with subsequent assessments of the vessel diameter performed manually²⁰ or using automated edge detection software^{21,22}. The use of GTN helps to determine if abnormalities in vasodilatation are due to a loss in smooth muscle cell integrity, or impaired release of NO from the endothelial cells²³. FMD and GTN are expressed as the percentage increase in post-stimulus vessel diameter relative to the baseline diameter.

The correct assessment of FMD requires a number of important considerations in the study protocol^{24,25}. The duration of cuff occlusion must be carefully timed; 5 min of cuff occlusion is sufficient for NO-mediated dilatation while longer cuff occlusion results in non-NO mediated dilatation²⁶. Similarly, placement of the occluding cuff around the wrist and distal from the ultrasound probe predominantly invokes NO-mediated dilatation, whereas cuff placement on the upper arm and proximal to the probe only partially stimulates NO²⁷. It is also important to measure peak dilatation following cuff deflation over a protracted period of time, as measurement of peak diameter within the first 60 sec following cuff deflation can underestimate FMD by 25 – 40%²⁸. Indeed, a period of 180 sec is likely to be sufficient in capturing true peak diameter, with most peak values occurring within the first 120 sec²⁸.

The stimulus for FMD involves the production of shear stress, which activates specific endothelial receptors to release NO²⁹. However, shear stress may also activate several other vasoactive factors (some of which may cause vasoconstriction)³⁰, making it essential that the evoked shear stress stimulus reflects vasodilatation from NO pathways²⁶. It is also important to account for the shear stress stimulus during FMD, with calculation of shear rate (velocity/diameter) serving as an adequate measure of shear stress, but not necessarily reflecting peak flow³¹. Recent physiological recommendations suggest that the shear stress profile should always be characterised when ultrasound systems allow simultaneous measurement of pulse wave velocity and active B-mode imaging in duplex mode²⁵.

Assessment of the carotid arteries using B-mode ultrasound can provide information on the carotid intima-media thickness (cIMT), and was first described in 1986 by Pignoli and colleagues³². Assessment of cIMT reflects proliferation of smooth muscle cells into the intima of the vessel and is a useful predictor of clinical events in early atherosclerosis³³. Carotid ultrasound can often predict arterial structure better than similar techniques (such as magnetic resonance imaging or radiographic assessments)³⁴. In addition, cIMT associates with a number of classical CVD risk factors including ageing, hypertension, and dyslipidemia³⁵. Changes to the walls of the carotid artery are usually initiated by a reduction in NO bioavailability which promotes inflammation within the vessel³⁶. The common carotid artery, internal carotid artery and carotid bifurcation points can be used to determine cIMT, as each site can similarly predict cardiovascular events³⁷.

In the present manuscript, we provide detailed methodology on assessment of microvascular endothelial function (LDI with iontophoresis), large vessel endothelial function (FMD and GTN) and vascular morphology (cIMT). Atherosclerosis is a multi-stage process which begins with endothelial dysfunction and ends with focal atherosclerotic lesions in the large arteries. The rationale for choosing the above assessments is that they reflect the different stages of atherosclerosis and help to account for the heterogeneous nature of the vasculature³⁸. Furthermore, we have previously shown that in a population of patients at increased risk for CVD, microvascular endothelial function was independent from large vessel endothelial function³⁹, and functional assessments were independent from structural assessments of the vasculature⁴⁰. Therefore, global assessments of the vasculature can help to decipher the different stages of atherosclerosis.

Protocol

NOTE: The protocol follows guidelines from Dudley Group NHS Foundation Trust's Human Research Ethics Committee. Perform all described techniques in a temperature controlled laboratory (21 – 22 °C), with stable lighting and absence of noise. Ask individuals undergoing assessments to refrain from food, drink, smoking and exercise 12 hr prior to the test. Withhold vasoactive medications for at least 12 hr when appropriate.

1. Laser Doppler Imaging with Iontophoresis

1. Switch on Laser Doppler Imager (LDI) and allow the scanner to automatically stabilise for approximately 30 min. Start the LDI software and click 'Measurement' (the software's home screen will then be shown). On the home screen, select 'Ionto Protocol' on the taskbar located at the top of the window.
2. Manually enter the protocol (the protocol used in our laboratory involves a total of 13 scans, with electrical current for iontophoretic drug delivery set from scan 2 to scan 11 at a voltage of 30 μ A). Set scan 1 as a baseline scan with no electric current, and scan 12 & 13 as recovery scans also with no electrical current. Click OK to confirm settings and return to home screen.
3. Ask participant to relax in a semi-recumbent chair with their forearm resting 90 degrees on a comfortable, firm pillow, and place a black mat under the forearm.
NOTE: The mat helps to limit artefact measurements generated by background surfaces surrounding the tissue. It is important that the participants arm is strapped firmly to the pillow so that there is no movement and associated artefacts.
4. Connect the wired plugs at the opposite end of each perspex chamber to the iontophoresis controller. Connect the chamber containing a 2.5 ml dose of 1% acetylcholine (ACh) to the anodal connection of the iontophoresis controller, and connect the second chamber containing a 2.5 ml dose of 1% sodium-nitroprusside (SNP) to the cathodal connection. Mix both agents in the chamber using 0.5% saline solution. Connect the two chambers to the volar aspect of the participant's right forearm using double sided adhesive pads.
5. Cover the chambers by 32 mm coverslips to prevent leakage of fluid.
6. Before starting the scan, open the 'Scanner Setup' window located on the top left of the home screen. Select the 'Video and Distance' tab and select the 'auto distance' function to measure the distance of the scanner head from the participants forearm.

1. Following completion of the auto distance measurement, select the 'Image Scan' tab and determine the area that is to be scanned by clicking the 'Mark' button in the bottom right corner of the window. If needed, change the size of the region of interest by manually entering in the size of the scanning area into the 'Scan Area' section near the top of the window. Ensure that the region of interest includes the diameter of each of the iontophoresis chambers and is large enough to limit variability in skin blood flow.
 7. Following completion of the assessment, save the data file. Open the data file using LDI image analysis software to perform measurements of perfusion.
 1. Click 'Image Review' on the main software window, and open the image file that is to be analysed.
 2. Use the software to mark out a region of interest around the outer diameters of each chamber. Adjust the region of interest so that it fits correctly on the area where the chambers were present. Then click the 'statistics' icon and a column containing the median perfusion units for each chamber will be displayed. Note the baseline perfusion unit, as well as the highest perfusion unit from each of the preceding 12 scans for each chamber.

NOTE: This method of analysis is specific to our laboratory; however, other methods can be used to express data obtained from the LDI scan. For a comprehensive review please refer to guidelines from Roustit and Cracowski ¹².
 8. To calculate percentage change in perfusion in response to ACh and SNP, subtract baseline perfusion from the peak perfusion, divide by baseline perfusion and then multiply by 100.
- NOTE: In our lab, changes in perfusion relative to baseline have shown good intra-observer coefficient of variation for ACh (7%) and SNP (6%).

2. Flow-mediated Dilatation and Glyceryl trinitrate-mediated Dilatation

1. Switch on the Doppler ultrasound machine and networked PC containing vascular image analysis (VIA) software.

NOTE: The VIA software captures a live image (at 25 frames per sec) and provides information on the vessel diameter as well as the quality of the vascular borders being detected by the ultrasound machine. Other software packages are available which may contain additional features and settings. It is advisable to consult operating manuals for specific software.
2. Ask participant to relax in a semi-recumbent armchair and place their arm on a comfortable pillow out to their side but level with the heart. Place a blood pressure cuff around the participant's wrist.

NOTE: The patient should be asked to keep their arm as still as possible to prevent movement artefacts during the measurement.
3. Secure the linear array transducer from the ultrasound machine into a stereotactic clamp, and tighten the clamp using the wingnuts so that the ultrasound transducer remains in a fixed position.

NOTE: The clamp will ensure that the ultrasound transducer will remain stable once the blood vessel is located.
4. On the ultrasound machine, scroll into the 'Menu' and set the scanning frequency at 5 MHz and optimize the depth (the recommended depth setting is 3.5 cm) and gain settings on the ultrasound machine. Adjust the gain settings to ensure that there is symmetrical brightness for the near and far wall of the vessel.
5. Using the linear array transducer, locate the brachial artery which is usually found 2-10 cm above the antecubital fossa in the longitudinal scanning plane. Make any adjustments to clarify the image quality at this stage. To help identify the artery, turn on the colour Doppler to help show pulsatile arterial blood flow and distinguish it from continuous venous blood flow. View the brachial artery horizontally across the screen; it should appear as two solid parallel lines, separated by a clear area in between the lines which represents the lumen of the vessel.
6. To allow the VIA software to automatically record vessel diameter, use the cursor to mark a predetermined region of interest to detect and track the anterior and posterior walls of the artery.

NOTE: The size of the region of interest can be increased or decreased using the 'x' and 'y' buttons located on the main software screen.
7. Click 'Start' on the VIA software and image the artery for 2 min. Following this, press 'Inflate' on the VIA software and simultaneously inflate the blood pressure cuff placed around the wrist to suprasystolic pressures (usually above 220 mmHg) for 5 min.

NOTE: The purpose of the wrist cuff is to occlude blood flow to the hand.
8. After 5 min deflate the blood pressure cuff to induce reactive hyperaemia which, in a healthy vessel, will stimulate NO-mediated vasodilatation.

NOTE: Peak dilatation can occur up to 180 sec following cuff deflation, so it is advisable to continue recording vascular diameters for 3 min after cuff release.
9. Following a 10 min rest period, re-locate the brachial artery using the linear array transducer and record a 2 min baseline diameter reading in the same manner as step 2.7.
10. Then ask the participant to place a 500 µg sublingual glyceryl-trinitrate (GTN) tablet under their tongue and continue to measure the brachial artery diameter for a further 5 min. After this period, ask the participant to remove the GTN tablet and monitor the participant to make sure they do not experience any adverse effects to the drug.
11. Carry out all analysis of data offline. Twenty-five data points are available for each second of the assessment; collapse this data into one-second epochs in Microsoft Excel. Export the data to a digital signal analysis package and filter with a 3 sec moving average filter.
12. Establish the baseline diameter from the 120 sec of data prior to the cuff-inflation. Visually inspect the baseline region and exclude artefacts. Average the remaining baseline regions to produce the baseline diameter.
13. For the flow-mediated dilatation (FMD) analysis, use the software to automatically scan the post cuff-deflation region for peak dilation and use the cursor to mark this peak for visual inspection. If the peak has been misidentified, use the cursor to select a more confined region within which the peak could then be identified. Record the peak value as peak diameter.
14. For the GTN data, adopt an identical procedure to that used with FMD, except search for peak dilation in the region following the 5 min of drug administration.
15. To calculate FMD % and GTN %, subtract baseline diameter from the peak diameter, divide by baseline diameter and then multiply by 100.

NOTE: In our laboratory, the intra-observer coefficient of variation is 11% for FMD, and 12% for GTN.

3. Carotid Intima-media Thickness

1. Ask participant to lie comfortably on a bed, and place a pillow under the head to offer support to the neck.

2. Connect the electrocardiogram (ECG) leads to the Doppler ultrasound and then attach them onto the patient limbs. Only a basic ECG trace is required, so place the appropriate leads on the left and right arms, and on the left ankle.
3. Prepare the ultrasound machine by scrolling through the 'menu' and setting the scanning frequency at 10 MHz and optimizing depth (the recommended depth setting is 3 – 4 cm) and gain settings. Adjust the gain settings to ensure that there is symmetrical brightness for the near and far wall of the vessel.
4. Ask participant to tilt their head slightly to the left, and using the linear array transducer, scan the right carotid artery along all its sections (common, internal and external carotid artery) using the longitudinal scanning plane to identify the presence of any plaques. Save images that display any evidence of plaque. To help identify the artery, look for a bifurcation point in the vessel, as this shows the common carotid artery bifurcating into the internal and external carotid arteries.
5. For measurement of carotid intima-media thickness (cIMT), attain at least 3 images of a section of the common carotid artery that is free of plaque, and is 1 cm proximal to the carotid bulb. Attain all images at the peak of the R wave on the ECG as this corresponds to ventricular diastole and the point at which the vessel is under the least amount of shear stress.
6. Repeat steps 3.4 and 3.5 in the left carotid artery. Ask the participant to tilt their head slightly to the right for this measurement.
7. To assist in attaining clear images of the near and far walls, carefully manipulate the ultrasound probe during the assessment to ensure the vessel is perpendicular to the ultrasound beam. Achieve this by subtly changing the tilt and rotation of the transducer along with minor adjustments to the pressure applied to the proximal-to-distal angle (heel-toe movement) of the probe.
8. Carry out analysis of images offline using Artery Measurement Software (AMS) to detect the vascular boundary according to the lines of Pignoli. Load up the image to be analyzed, and then using the cursor, create a region of interest in a section of the vessel that is free from plaque. Click 'detect' on the software and record the values displayed on the screen for cIMT and lumen diameter.
NOTE: accurate readings can only be obtained from the far wall, so ignore readings from the near wall.
9. Take three measurements for each side, and then average these to give the mean cIMT for the right and left carotid arteries separately. Further average the cIMT from both sides to give the overall cIMT.
NOTE: The intra-observer coefficient of variation for this technique in our laboratory is 9%.
10. Perform measurement of any plaque using the same software by manually marking out the plaque using the cursor. Click 'classify' on AMS to automatically calculate the echogenicity of the plaque and grade according to its susceptibility for rupture. Click on the "Plaque Characteristics" window to see this information.

Representative Results

Laser Doppler Imaging with Iontophoresis

The median blood flux units following the laser Doppler imaging scans from a healthy middle aged female free from CVD are shown in **Figure 1**. There was a marked increase in median blood flux for both ACh and SNP. Baseline blood flux was 48 perfusion units for ACh, and 67 perfusion units for SNP. Peak blood flux in response to ACh was 455 perfusion units, and for SNP 446 perfusion units. This yielded an 831% and 566% increase in perfusion (relative to baseline) for ACh and SNP respectively. The values that are provided are highly-dependent on the equipment used to examine skin blood flux along with environmental factors.

Flow-mediated dilatation and Glyceryl trinitrate-mediated Dilation

Figure 2 displays the baseline and peak diameters for FMD and GTN assessments from a healthy young male free from CVD. The baseline diameter of the brachial artery was 3.0 mm for the FMD and GTN assessments. The peak diameter in the FMD test was 3.3 mm, while for the GTN assessment it was 3.9 mm, which corresponds to a 10 and 30% increase in blood flow respectively, relative to baseline.

Carotid Intima-media Thickness

Figure 3 shows the left carotid artery of a healthy individual. Calculation of cIMT values is performed using automated edge-detection software. The cIMT in the far wall was 0.83mm and the lumen diameter of the vessel was 7.71mm. The results for the right carotid artery in the same individual were 0.87mm for cIMT, and 7.80mm for the lumen diameter. When averaging the reading from both sides, cIMT was 0.85mm, and lumen diameter was 7.76mm.

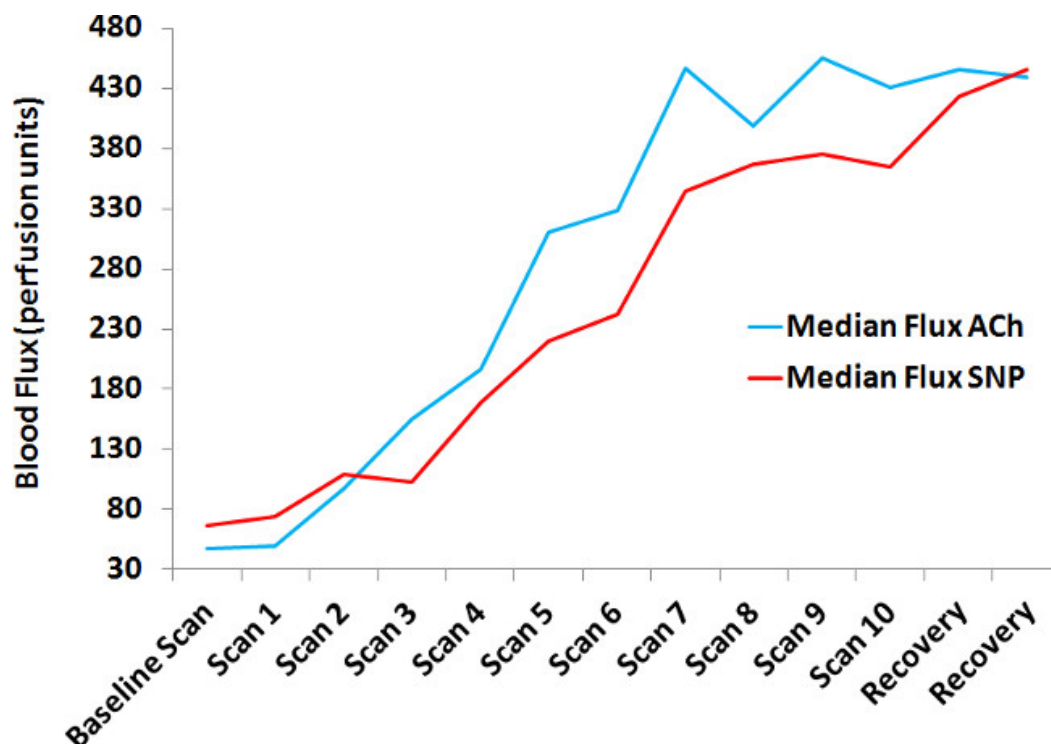


Figure 1. Changes in blood flux in response to laser Doppler imaging with iontophoresis. After completion of a baseline scan to measure baseline blood flux, 10 scans (scan 1 to 10) with iontophoresis of ACh and SNP using a 30 μ a electrical current were performed. Following iontophoresis, 2 recovery scans were performed. ACh = acetylcholine; SNP = sodium nitroprusside.

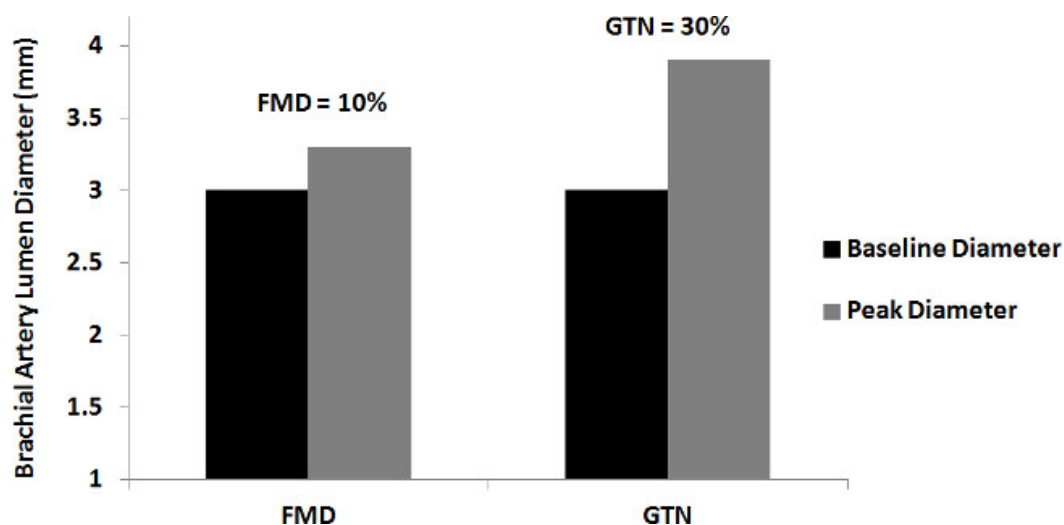


Figure 2. Flow-mediated and glyceryl trinitrate-mediated dilatation. The graph displays the baseline diameter and a clear increase in peak diameters following application of the flow-mediated and glyceryl trinitrate-mediated dilatation stimuli. FMD = flow-mediated dilatation; GTN = glyceryl trinitrate-mediated dilatation.

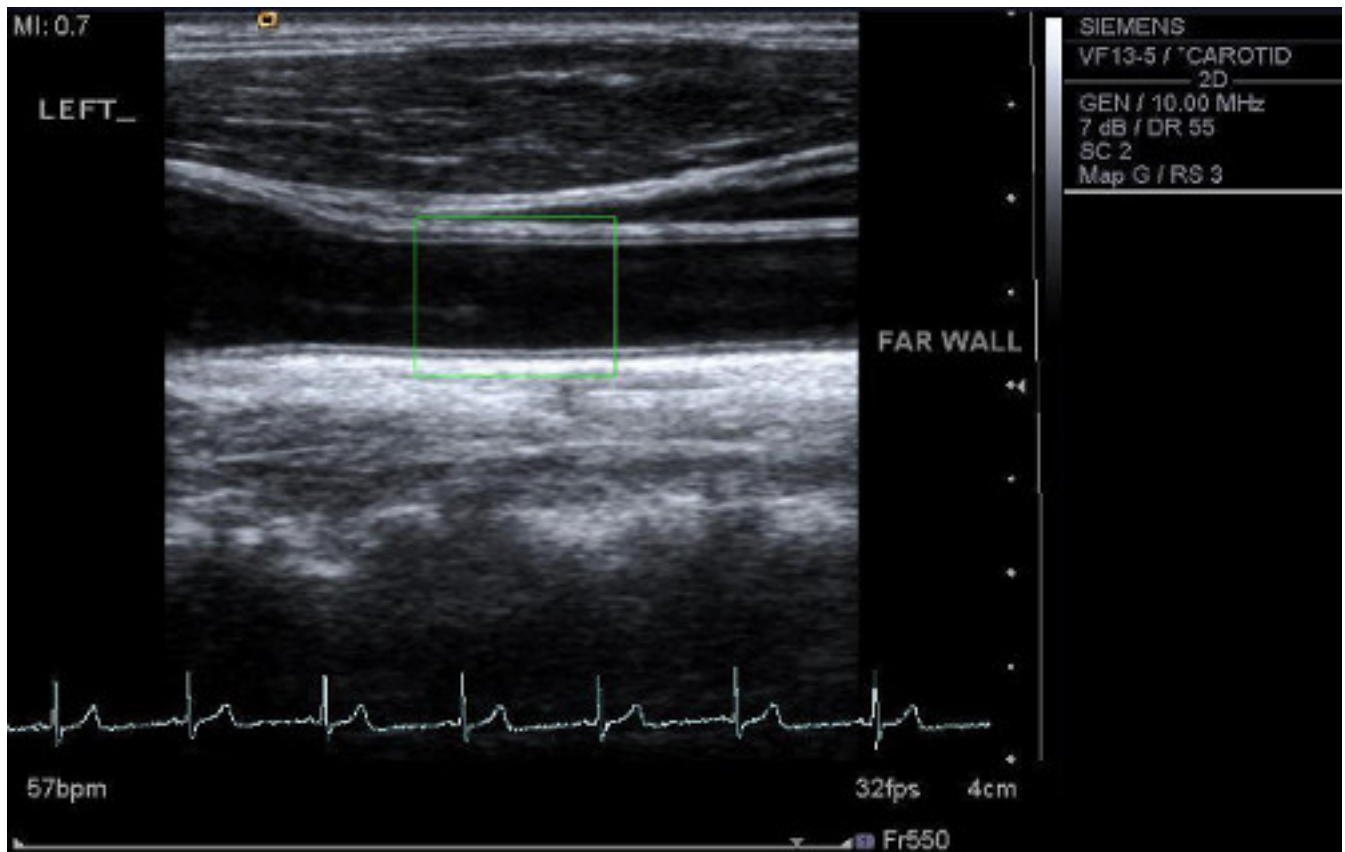


Figure 3. Ultrasound scan of the carotid artery. An ultrasound scan of the left carotid artery is shown with a region of interest placed 1cm from the carotid bulb (point of bifurcation). [Please click here to view a larger version of this figure.](#)

Discussion

The present manuscript details the methodology of several distinct assessments of vascular function and morphology which can be performed in the peripheral vasculature. Each assessment provides information on the distinct stages of atherosclerosis, and help to characterize the vascular profile of different vascular territories.

We have previously reported that microvascular endothelial function is independent from large vessel endothelial function in a population of rheumatoid arthritis patients at increased risk of CVD³⁹. Moreover, assessments of vascular function and morphology were also independent from each other in the same group of patients and in patients with CVD^{40,41}. These findings can be explained by the heterogeneity of function and structure of endothelial cells in different vascular territories³⁸, as well as a possible time lag for progression of functional alterations to morphological abnormalities in the vessel. A study by Hashimoto and colleagues⁴² revealed that several participants with atherosclerosis had decreased FMD values but normal cIMT values. These findings suggest that examination of subclinical atherosclerosis using a variety of methods is important to decipher the global effects of CVD.

The importance of the microvasculature in health and disease is gaining increasing attention in the medical literature. The microvessels form a much larger surface area than large vessels making them significant targets for damage from injurious stimuli⁴³. It has been hypothesized that microvessels might be the primary source of inflammatory mediators which infiltrate the endothelium of the larger vessels leading to lesion formation⁴³. In type II diabetics, microvascular disease often precedes large vessel disease⁴⁴, and in other populations with increased risk for CVD such as rheumatoid arthritis, interventions which reduce the CVD risk improve microvascular, but not large vessel, endothelial function^{45,46}. Collectively, these findings suggest that examination of microvascular function may help in understanding the complex mechanisms which initiate atherosclerosis.

In the present work, assessment of microvascular endothelial function was performed using LDI with iontophoresis of vasoactive agents. Several other assessments can be used to assess microvascular function including nailfold capillaroscopy and venous occlusion plethysmography. However, the former assessment provides information on microvascular morphology only, while the latter is time consuming and in some protocols invasive due to administration of intra-brachial vasoactive agents¹. In contrast, LDI offers a simple, time-efficient approach to measure microvascular perfusion of skin blood vessels in response to vasoactive agents which are administered non-invasively. The measurement of skin blood flow has gained widespread acceptance in the literature due to its ease of accessibility and strong correlation with established CVD¹². Moreover, the advantage of LDI over other Doppler techniques such as laser Doppler flowmetry, is that it can simultaneously scan multiple points in a given area and can therefore account for cellular movement artefacts and spatial differences of skin blood flow, both of which can affect the perfusion of the vessel^{47,48}.

Despite the obvious advantages of iontophoresis, it is important to note that current induced vasodilatation (CIV) from iontophoresis may confound the effects of the vasoactive agents especially at the cathode. The choice of vehicle for drug delivery could help to reduce this effect, with 0.5% sodium chloride (as used in the current protocol) effective in limiting CIV¹⁸. Furthermore, use of larger diameter chambers and low electrical currents (as used in the current protocol) all help to reduce CIV¹⁸. Use of a control site has also been recommended¹². Biological and behavioural factors can also affect the reliability and repeatability of the technique. For example, circadian variation and smoking have been shown to influence microvascular endothelial function^{49,50}. Strict recording conditions must be adhered to in order to obtain accurate results and established guidelines should be followed when designing protocols¹².

Measurement of FMD and GTN-mediated dilatation provides information on endothelial dysfunction in the large blood vessels, and is used widely in non-invasive vascular research. The FMD technique provides surrogate information on NO bioavailability and is a useful prognostic marker of cardiac events in different clinical populations⁷⁻⁹. In the present work, the protocol presented accounts for many of the factors that are necessary for adequate stimulation of NO-mediated vasodilatation²⁵. For example, the occluding cuff was placed distal to the ultrasound probe and around the wrist²⁷, the duration of ischemia was 5 min²⁶ and adequate time was allowed to record the 'true' peak diameter following reactive hyperaemia²⁸. Unfortunately, the protocol did not include characterization of the shear stress profile as the automatic edge detection software did not allow simultaneous recording of vessel diameter and pulse wave velocity signal. The calculation of shear stress is integral to accurate measurement of FMD²⁶ and we recommended that, where possible, vascular research groups use software which allows such measurements to be performed.

Assessments of FMD and GTN-mediated dilatation are also susceptible to environmental and biological variations²⁴, as small changes in vascular diameter can elicit large FMD/GTN responses. For example, typical FMD values for healthy participants range from 5-10%⁵¹, which corresponds to a 0.25 – 0.5mm change in arterial diameter for an artery with a diameter of 5mm. Given such small changes to the arterial diameter, careful attention must be paid to technical and biological factors that may influence the measurement. Indeed, FMD can be affected by a variety of biologic and behavioural factors such as sympathetic activation⁵², sleep deprivation⁵³, caffeine consumption⁵⁴, smoking⁵⁵, antioxidant therapy⁵⁶ and time of day⁵⁷. Accordingly, it is important to control for these factors by utilising information from established guidelines^{24,25}.

Assessment of advanced but subclinical atherosclerosis was done using cIMT. The technique has been utilised in several clinical populations and provides great detail on arterial structure when compared to more sophisticated techniques such as magnetic resonance imaging³⁴. As with the other vascular techniques, measurement of cIMT requires careful consideration of technical factors which can affect the measurement. Generally, cIMT should be performed in areas free from plaque, in the far wall of the common carotid artery. Similar to FMD, measurement of cIMT is performed using high-resolution ultrasonography and so is highly user-dependent. Reported coefficient of variation (CofV) range from 2.4 – 18.3%⁵⁸, while for FMD it is 1 – 84%⁵⁹. However, even when both techniques are performed by competent ultrasonographers with external factors well-controlled, there remains a high CofV^{58,60,61}. One reason for this could be that analysis of vascular borders are carried out using manual methods^{60,61}. Such analysis can reduce reliability as imaging artefacts such as false borders, noise from the ultrasound signal, and distortion of vessels can affect interpretation of the image²².

Recent developments in continuous automated edge-detection software have greatly improved the detection of vascular wall boundaries^{21,22}. In the present study, VIA software was used to measure the brachial artery diameter, while AMS was used to detect cIMT. The use of these software greatly reduces operator dependence, yet in the case of AMS, some degree of operator control is still available in situations where image quality may be poor⁶². Laboratories which use automated edge detection software generally tend to have low CofV^{58,63,64}, thus it should be the aim of all vascular research laboratories to incorporate automated measurement of vascular boundaries in order to ensure accuracy of the results. It is also good practice to report results of reproducibility studies for specific protocols when publishing study outcomes.

Although assessments of vascular function are routinely used in clinical research, a limitation of the techniques is that normative values for LDI with iontophoresis and FMD do not exist. It is therefore important that healthy age- and sex-matched control groups are examined to compare findings with the experimental group. Even though these techniques associate with poor prognosis in a variety of populations with evidence of CVD⁶⁻⁹, there is still a dearth of studies which have examined the relationship between poor endothelial function and adverse cardiovascular outcomes such as myocardial infarction and stroke. Further prospective studies are required to address these concerns. Another limitation is the use of human operators to perform the assessments and carry out the analysis. This introduces a potential source of bias; however, this can be limited by blinding the operator to the results or ensuring that the reader is different from the operator. It is also important to ensure that the reader follows a standardised protocol for data analysis, so that all data is analysed consistently.

In summary, the present manuscript provides detailed information on the methodological steps necessary to successfully perform assessments of microvessel and large vessel endothelial function as well as vascular morphology of the peripheral circulation. When used together, the assessments provide global information on the different stages of atherosclerosis. Further prospective studies examining the potential diagnostic role of these techniques are warranted.

Disclosures

The authors declare that they have no competing financial interests.

Acknowledgements

The authors would like to thank Dr George Balanos for his assistance in the flow-mediated dilatation technique.

References

1. Sandoo, A., Veldhuijzen van Zanten, J. J. C. S., Metsios, G. S., Carroll, D., Kitas, G. D. The endothelium and its role in regulating vascular tone. *The Open Cardiovascular Medicine Journal*. **4**, 302-312 (2010).
2. Lerman, A., Zeiher, A. M. Endothelial Function: Cardiac Events. *Circulation*. **111**, (3), 363-368 (2005).
3. Anderson, T. J., et al. Close relation of endothelial function in the human coronary and peripheral circulations. *Journal of American College of Cardiology*. **26**, (5), 1235-1241 (1995).
4. Takase, B., et al. Close relationship between the vasodilator response to acetylcholine in the brachial and coronary artery in suspected coronary artery disease. *International Journal of Cardiology*. **105**, (1), 58-66 (2005).
5. Khan, F., Patterson, D., Belch, J. J., Hirata, K., Lang, C. C. Relationship between peripheral and coronary function using laser Doppler imaging and transthoracic echocardiography. *Clinical Science (Lond)*. **115**, (9), 295-300 (2008).
6. Rossi, R., Nuzzo, A., Origliani, G., Modena, M. G. Prognostic role of flow-mediated dilation and cardiac risk factors in post-menopausal women. *Journal of American College of Cardiology*. **51**, (10), 997-1002 (2008).
7. Brevetti, G., Silvestro, A., Schiano, V., Chiariello, M. Endothelial dysfunction and cardiovascular risk prediction in peripheral arterial disease: additive value of flow-mediated dilation to ankle-brachial pressure index. *Circulation*. **108**, (17), 2093-2098 (2003).
8. Gokce, N., et al. Predictive value of noninvasively determined endothelial dysfunction for long-term cardiovascular events in patients with peripheral vascular disease. *Journal of Cardiology*. **41**, (10), 1769-1775 (2003).
9. Jadhav, U. M., Sivaramakrishnan, A., Kadam, N. N. Noninvasive assessment of endothelial dysfunction by brachial artery flow-mediated dilatation in prediction of coronary artery disease in Indian subjects. *Indian Heart Journal*. **55**, (1), 44-48 (2003).
10. Ross, R. Atherosclerosis - an inflammatory disease. *The New England Journal of Medicine*. **340**, 115-126 (1999).
11. Celermajer, D. S., Sorensen, K. E., Bull, C., Robinson, J., Deanfield, J. E. Endothelium-dependent dilation in the systemic arteries of asymptomatic subjects relates to coronary risk factors and their interaction. *Journal of American College of Cardiology*. **24**, (6), 1468-1474 (1994).
12. Roustit, M., Cracowski, J. L. Assessment of endothelial and neurovascular function in human skin microcirculation. *Trends in Pharmacological Sciences*. **34**, (7), 373-384 (2013).
13. Ahn, H., Johansson, K., Lundgren, O., Nilsson, G. E. In vivo evaluation of signal processors for laser Doppler tissue flowmeters. *Medical & Biological Engineering & Computing*. **25**, (2), 207-211 (1987).
14. Kalia, Y. N., Naik, A., Garrison, J., Guy, R. H. Iontophoretic drug delivery. *Advanced Drug Delivery Reviews*. **56**, (5), 619-658 (2004).
15. Morris, S. J., Shore, A. C. Skin blood flow responses to the iontophoresis of acetylcholine and sodium nitroprusside in man: possible mechanisms. *Journal of Physiology*. **496**, (Pt 2), 531-542 (1996).
16. Sandoo, A., Veldhuijzen van Zanten, J. J. C. S., Metsios, G. S., Carroll, D., Kitas, G. D. Vascular function and morphology in rheumatoid arthritis: a systematic review. *Rheumatology*. **50**, (11), 2125-2139 (2011).
17. Metsios, G. S., et al. Individualised exercise improves endothelial function in patients with rheumatoid arthritis. *Annals of Rheumatic Diseases*. **73**, (4), 748-751 (2014).
18. Ferrell, W. R., et al. Elimination of electrically induced iontophoretic artefacts: implications for non-invasive assessment of peripheral microvascular function. *Journal of Vascular Research*. **39**, (5), 447-455 (2002).
19. Khan, F., Newton, D. J., Smyth, E. C., Belch, J. J. F. Influence of vehicle resistance on transdermal iontophoretic delivery of acetylcholine and sodium nitroprusside in humans. *Journal of Applied Physiology*. **97**, (3), 883-887 (2004).
20. Celermajer, D. S., et al. Non-invasive detection of endothelial dysfunction in children and adults at risk of atherosclerosis. *Lancet*. **340**, (8828), 1111-1115 (1992).
21. Sidhu, J. S., Newey, V. R., Nassiri, D. K., Kaski, J. C. A rapid and reproducible on line automated technique to determine endothelial function. *Heart*. **88**, (3), 289-292 (2002).
22. Sonka, M., Liang, W., Lauer, R. M. Automated analysis of brachial ultrasound image sequences: early detection of cardiovascular disease via surrogates of endothelial function. *IEEE Transactions on Medical Imaging*. **21**, (10), 1271-1279 (2002).
23. Vallance, P., Collier, J., Moncada, S. Effects of endothelium-derived nitric oxide on peripheral arteriolar tone in man. *Lancet*. **2**, (8670), 997-1000 (1989).
24. Corretti, M. C., et al. Guidelines for the ultrasound assessment of endothelial-dependent flow-mediated vasodilation of the brachial artery: A report of the International Brachial Artery Reactivity Task Force. *Journal of American College of Cardiology*. **39**, (2), 257-265 (2002).
25. Thijssen, D. H., et al. Assessment of flow-mediated dilation in humans: a methodological and physiological guideline. *American Journal of Physiology - Heart and Circulatory Physiology*. **300**, (1), H2-H12 (2011).
26. Mullen, M. J., et al. Heterogenous Nature of Flow-Mediated Dilatation in Human Conduit Arteries In Vivo : Relevance to Endothelial Dysfunction in Hypercholesterolemia. *Circulation Research*. **88**, (2), 145-151 (2001).
27. Doshi, S. N., et al. Flow-mediated dilatation following wrist and upper arm occlusion in humans: the contribution of nitric oxide. *Clinical Sciences (Lond)*. **101**, (6), 629-635 (2001).
28. Black, M. A., Cable, N. T., Thijssen, D. H., Green, D. J. Importance of measuring the time course of flow-mediated dilatation in humans. *Hypertension*. **51**, (2), 203-210 (2008).
29. Traub, O., Berk, B. C. Laminar Shear Stress : Mechanisms by Which Endothelial Cells Transduce an Atheroprotective Force. *Arteriosclerosis, Thrombosis, and Vascular Biology*. **18**, (5), 677-685 (1998).
30. Pyke, K. E., Tschakovsky, M. E. The relationship between shear stress and flow-mediated dilatation: implications for the assessment of endothelial function. *The Journal of Physiology Online*. **568**, (2), 357-369 (2005).
31. Pyke, K. E., Dwyer, E. M., Tschakovsky, M. E. Impact of controlling shear rate on flow-mediated dilation responses in the brachial artery of humans. *Journal of Applied Physiology*. **97**, (2), 499-508 (2004).
32. Pignoli, P., Tremoli, E., Poli, A., Oreste, P., Paoletti, R. Intimal plus medial thickness of the arterial wall: a direct measurement with ultrasound imaging. *Circulation*. **74**, (6), 1399-1406 (1986).
33. Corrado, E., et al. Endothelial dysfunction and carotid lesions are strong predictors of clinical events in patients with early stages of atherosclerosis: a 24-month follow-up study. *Coronary Artery Disease*. **19**, (3), 139-144 (2008).

34. Touboul, P. J., *et al.* Mannheim carotid intima-media thickness and plaque consensus (2004-2006-2011). An update on behalf of the advisory board of the 3rd, 4th and 5th watching the risk symposia, at the 13th, 15th and 20th European Stroke Conferences, Mannheim, Germany, 2004, Brussels, Belgium, 2006, and Hamburg, Germany, 2011. *Cerebrovascular Disease*. **34**, (4), 290-296 Mannheim, Germany (2012).
35. Oren, A., Vos, L. E., Uiterwaal, C. S. P. M., Grobbee, D. E., Bots, M. L. Cardiovascular Risk Factors and Increased Carotid Intima-Media Thickness in Healthy Young Adults: The Atherosclerosis Risk in Young Adults (ARYA) Study. *Archives of Internal Medicine*. **163**, (15), 1787-1792 (2003).
36. Wohlin, M., *et al.* Both cyclooxygenase- and cytokine-mediated inflammation are associated with carotid intima-media thickness. *Cytokine*. **38**, (3), 130-136 (2007).
37. Iglesias del, S. a, Bots, M. L., Grobbee, D. A., Hofman, A., Witteman, J. C. Carotid intima-media thickness at different sites: relation to incident myocardial infarction; The Rotterdam Study. *European Heart Journal*. **23**, (12), 934-940 (2002).
38. Aird, W. C. Phenotypic heterogeneity of the endothelium: II. Representative vascular beds. *Circulation Research*. **100**, (2), 174-190 (2007).
39. Sandoo, A., Carroll, D., Metsios, G. S., Kitas, G. D., Veldhuijzen van Zanten, J. J. The association between microvascular and macrovascular endothelial function in patients with rheumatoid arthritis: a cross-sectional study. *Arthritis Research and Therapy*. **13**, (3), R99 (2011).
40. Sandoo, A., Hodson, J., Douglas, K. M., Smith, J. P., Kitas, G. D. The association between functional and morphological assessments of endothelial function in patients with rheumatoid arthritis: a cross-sectional study. *Arthritis Research and Therapy*. **15**, (5), R107 (2013).
41. Rohani, M., Jogestrand, T., Kallner, G., Jussila, R., Agewall, S. Morphological changes rather than flow-mediated dilatation in the brachial artery are better indicators of the extent and severity of coronary artery disease. *Journal of Hypertension*. **23**, (7), 1397-1402 (2005).
42. Hashimoto, M., *et al.* Correlation between flow-mediated vasodilatation of the brachial artery and intima-media thickness in the carotid artery in men. *Arteriosclerosis, Thrombosis, and Vascular Biology*. **19**, (11), 2795-2800 (1999).
43. Stokes, K. Y., Granger, D. N. The microcirculation: a motor for the systemic inflammatory response and large vessel disease induced by hypercholesterolaemia. *Journal of Physiology*. **562**, (Pt 3), 647-653 (2005).
44. Krentz, A. J., Clough, G., Byrne, C. D. Vascular disease in the metabolic syndrome: do we need to target the microcirculation to treat large vessel disease). *Journal of Vascular Research*. **46**, (6), 515-526 (2009).
45. Sandoo, A., *et al.* Anti-TNFalpha therapy may lead to blood pressure reductions through improved endothelium-dependent microvascular function in patients with rheumatoid arthritis. *Journal of Human Hypertension*. **25**, (11), 699-702 (2011).
46. Sandoo, A., van Zanten, J. J., Toms, T. E., Carroll, D., Kitas, G. D. Anti-TNFalpha therapy transiently improves high density lipoprotein cholesterol levels and microvascular endothelial function in patients with rheumatoid arthritis: a pilot study. *BMC. Musculoskeletal Disorders*. **13**, 127 (2012).
47. Wardell, K., Jakobsson, A., Nilsson, G. E. Laser Doppler perfusion imaging by dynamic light scattering. *The IEEE Transactions on Biomedical Engineering*. **40**, (4), 309-316 (1993).
48. Line, P. D., Mowinckel, P., Lien, B., Kvernebo, K. Repeated measurement variation and precision of laser Doppler flowmetry measurements. *Microvascular Research*. **43**, (3), 285-293 (1992).
49. Elherik, K., Khan, F., McLaren, M., Kennedy, G., Belch, J. J. F. Circadian variation in vascular tone and endothelial cell function in normal males. *Clinical Science*. **102**, (5), 547-552 (2002).
50. Pellaton, C., Kubli, S., Feihl, F., Waeber, B. Blunted vasodilatory responses in the cutaneous microcirculation of cigarette smokers. *American Heart Journal*. **144**, (2), 269-274 (2002).
51. Moens, A. L., Goovaerts, I., Claeys, M. J., Vrints, C. J. Flow-Mediated Vasodilation: A Diagnostic Instrument, or an Experimental Tool. *Chest*. **127**, (6), 2254-2263 (2005).
52. Hijmering, M. L., *et al.* Sympathetic activation markedly reduces endothelium-dependent, flow-mediated vasodilation. *Journal of the American College of Cardiology*. **39**, (4), 683-688 (2002).
53. Takase, B., Akima, T., Uehata, A., Ohsuzu, F., Kurita, A. Effect of chronic stress and sleep deprivation on both flow-mediated dilation in the brachial artery and the intracellular magnesium level in humans. *Clinical Cardiology*. **27**, (4), 223-227 (2004).
54. Papamichael, C. M., *et al.* Effect of coffee on endothelial function in healthy subjects: the role of caffeine. *Clinical Sciences(Lond)*. **109**, (1), 55-60 (2005).
55. Lekakis, J., *et al.* Effect of acute cigarette smoking on endothelium-dependent brachial artery dilatation in healthy individuals). *American Journal of Cardiology*. **79**, (4), 529-531 (1997).
56. Engler, M. M., *et al.* Antioxidant Vitamins C and E Improve Endothelial Function in Children With Hyperlipidemia: Endothelial Assessment of Risk from Lipids in Youth. *Circulation*. **108**, (9), 1059-1063 (2003).
57. Etsuda, H., *et al.* Morning attenuation of endothelium-dependent, flow-mediated dilation in healthy young men: possible connection to morning peak of cardiac events. *Clinical Cardiology*. **22**, (6), 417-421 (1999).
58. Kanfers, S. D., Algra, A., van Leeuwen, M. S., Banga, J. D. Reproducibility of in vivo carotid intima-media thickness measurements: a review. *Stroke*. **28**, (3), 665-671 (1997).
59. West, S. G., *et al.* Biological correlates of day-to-day variation in flow-mediated dilation in individuals with Type 2 diabetes: a study of test-retest reliability. *Diabetologia*. **47**, (9), 1625-1631 (2004).
60. Roos, N. M., Bots, M. L., Schouten, E. G., Katan, M. B. Within-subject variability of flow-mediated vasodilation of the brachial artery in healthy men and women: implications for experimental studies. *Ultrasound in Medicine and Biology*. **29**, (3), 401-406 (2003).
61. Tyldum, E. V., Madssen, E., Skogvoll, E., Slordahl, S. A. Repeated image analyses improves accuracy in assessing arterial flow-mediated dilatation. *Scandinavian Cardiovascular Journal*. **42**, (5), 310-315 (2008).
62. Liang, Q., Wendelhag, I., Wikstrand, J., Gustavsson, T. A multiscale dynamic programming procedure for boundary detection in ultrasonic artery images. *The IEEE Transactions on Biomedical Engineering*. **19**, (2), 127-142 (2000).
63. Hijmering, M. L., *et al.* Variability of flow mediated dilation: consequences for clinical application. *Atherosclerosis*. **157**, (2), 369-373 (2001).
64. Woodman, R. J., *et al.* Improved analysis of brachial artery ultrasound using a novel edge-detection software system. *Journal of Applied Physiology*. **91**, (2), 929-937 (2001).